α decay and shape coexistence in the α-rotor model

J. D. Richards,[1] T. Berggren,[2,3,*] C. R. Bingham,[1,4] W. Nazarewicz[1,4,5] and J. Wauters[1]
[1]*Department of Physics & Astronomy, University of Tennessee, Knoxville, Tennessee 37996*
[2]*Department of Mathematical Physics, Lund Institute of Technology, P.O. Box 118, S-22100 Lund, Sweden*
[3]*Joint Institute of Heavy Ion Research, Oak Ridge National Laboratory, P.O. Box 2008, Oak Ridge, Tennessee 37831*
[4]*Physics Division, Oak Ridge National Laboratory, P.O. Box 2008, Oak Ridge, Tennessee 37831*
[5]*Institute of Theoretical Physics, Warsaw University, Hoża 69, PL-00681, Warsaw, Poland*
(Received 18 November 1996)

The particle-plus-rotor model was employed to study the fine structure seen in the α decay of even-even neutron-deficient nuclei in the Hg-Po region. The configuration mixing resulting from the shape coexistence between well-deformed prolate bands and spherical (or quasirotational oblate) structures in the daughter nuclei was considered. Experimental α-decay branching ratios are reproduced within one order of magnitude, except for the case of ^{180}Hg, where the daughter nucleus ^{176}Pt is expected to be triaxial in its ground state. The effect of configuration mixing on the relative intensities is discussed in detail, together with the sensitivity of results to the choice of the α-nucleus optical model parameters. [S0556-2813(97)04609-8]

PACS number(s): 21.60.−n, 23.60.+e, 24.10.Ht, 27.80.+w

I. INTRODUCTION

Alpha decay has proved to be a very powerful tool to observe heavy neutron-deficient nuclei and study their structure. The idea that an α particle is first formed inside the nucleus (preformation) and then tunnels through an effective potential barrier of the daughter system was described quantum mechanically by Gamow [1] and Condon and Gurney [2]. Rasmussen [3] utilized the real part of the α-nucleus optical potential in the surface region, derived from elastic α-scattering experiments [4], to calculate the tunneling through the Coulomb and centrifugal barriers. Later, the phenomenon of α decay was given a microscopic description by means of the nuclear shell model; this approach was able to reproduce relative α widths for Po and odd-At isotopes in the $N=126$ region [5]. However, the shell model calculations yielded absolute α-decay widths which were orders of magnitude too small compared to the experimental values, the main reason being an improper treatment of the continuum. Although configuration mixing effects were incorporated at a later stage, they still could not account completely for the discrepancy with the data. Today it is understood that the crucial role in the α-particle formation process is played by strong correlations between two-particle states, associated with high-lying shell-model configurations and giving rise to strong clustering near the nuclear surface (see the recent review [6]).

In a series of works based on general reaction theory, the partial width of the α decay was estimated for spherical nuclei using a two potential approach [7–10] (see also Sec. II B of Ref. [6] and references quoted therein). This theory was applied to the deformed case by Berggren and Olanders [11] who introduced an α-plus-rotor model. They assumed that the α-nucleus interaction, in addition to a spherical central potential, contains the rotationally invariant quadrupole-quadrupole component. This model has recently been applied to half-lives and angular anisotropies in the α decay of some odd Rn, Fr, Pa, and U isotopes [12].

Buck *et al.* [13], in a simple spherical semiclassical treatment, succeeded in reproducing all α-decay constants of the even-even α emitters, and were able to describe the favored α decays of odd nuclei. Following the method introduced in Ref. [14], the semiclassical approach has recently been applied to describe the α-decay branching ratios of even-even actinide nuclei [15].

The absolute α-decay widths of lead isotopes, including the radial dependence of the formation amplitude, were calculated within a realistic shell-model-based approach in a large configuration space [16–18]. Absolute α-decay widths have also been calculated in axially symmetric shapes and applied to deformed even-even [19,20] and odd-mass *trans*-lead nuclei [21,22].

In the lead region, manifestations of shape coexistence are by now clearly established in a large number of nuclei [23,24]. In the neutron-deficient even-even Pt, Hg, Pb [23], and recently also in Po nuclei [25], intruder 0^+ states (often with rotational-like structures built upon them) occur at low excitation energy. In the Hg and Pb isotopes, the excited intruder configuration is believed to be more deformed than the ground-state configuration, and the excitation energy of the deformed band reaches a minimum near midshell. In the neutron-deficient Pt isotopes, the deformed intruder configuration becomes the ground state and the excited 0^+ states can be associated with quasirotational oblate structures [23]. In many cases the well-deformed prolate and weakly deformed oblate bands strongly interact and this gives rise to a strong configuration mixing. It was shown that the α decay to the 0^+ bandhead of the strongly deformed band is sensitive to the proton-pair configurations of the connecting states [26] and to the configuration mixing amplitudes [27]. A microscopic description of the intruder 0_2^+ states in Pb isotopes and their α feeding was performed in the framework of the random phase approximation (RPA), including proton-

*Deceased.

neutron pairing vibrations [28,29]; the calculated α-decay hindrance factors turned out to be in good agreement with experimental data.

The objective of this paper is twofold. First, we generalize the α-core model of Ref. [11] to the case of band mixing. Second, we demonstrate that configuration mixing due to the shape-coexistence effects does influence the fine structure seen in the α decay. Partial widths for α decay to excited states are calculated and the corresponding branching ratios

$$B(q)=\frac{\omega_q}{\Sigma_{q'}\omega_{q'}} \tag{1}$$

are determined. [In Eq. (1) $\omega_q=\Gamma_q/\hbar$ stands for the decay width to a particular excited state in a daughter nucleus characterized by the set of quantum numbers q.]

The paper is organized as follows. Section II contains the description of the theory, including a number of new features pertinent to the region discussed. The method used for computing the interaction between coexisting bands is discussed in Sec. III. The results of calculations are presented in Sec. IV. Finally, conclusions are contained in Sec. V.

II. FORMALISM

A quantal formulation of the theory of α decay of deformed and/or oriented nuclei based on a reaction-theoretical foundation was proposed some years ago [11]. The original version, implementing the idea of an α-particle-plus-rotor model with quadrupole-quadrupole coupling between the deformed core and the α particle, used a harmonic-oscillator basis for the single-particle α orbitals. This program was later employed to analyze the anisotropy measurement data [30] for odd-mass At and Po isotopes [31]. A more recent version, based on Woods-Saxon (WS) wave functions, was first used [32] to reanalyze the same data so as to confirm the applicability of the model to a number of light actinides, especially those showing indications of octupole deformation. It is important to stress that the model is basically a phenomenological one. The formulation in terms of the particle-rotor model is dictated by the need to take angular momentum conservation (rotational invariance) into account. When applying to realistic cases, empirical data must be used to fix the parameters of the model. Thus, for instance, potential depths must be adjusted so as to reproduce the decay energy (Q_α value) as given by empirical nuclide masses, because this energy has a very strong influence on the decay rate (or equivalently the half-life) of the nucleus considered. The theoretical validity of the model is to be sought in its ability to use general quantal principles and structural ideas to reveal relationships between different pieces of empirical data. On the other hand, the phenomenological nature of the model implies that it cannot be used for predicting, e.g., the half-life for a parent nucleus if either its mass or that of the daughter is unknown, and the model is unreliable for calculating intensity relations if the low-lying states of the daughter nucleus are unknown. It must also be pointed out that the Pauli principle can only be imposed in an approximate way because the α particle, a composite system, is treated as a pointlike object.

A. Alpha-core Hamiltonian

Consider a system A (the nucleus ${}^AZ$) formed by a spheroidal core C and an α particle. The interaction between the center of mass of the core and the α particle is expressed as a sum of a spherical α-core central potential $U(r)$ and the multipole-multipole term describing the coupling between the multipole moment of the core, $Q^{\lambda}_{Cm}(\Omega)$, and that of the α orbital, $Q^{\lambda}_m(\mathbf{r})$. Under these assumptions, the α-core Hamiltonian can be written as

$$H_A=H_C+H_\alpha+T_\alpha+U(r)+V_{QQ}, \tag{2}$$

where H_C and H_α are the intrinsic Hamiltonians of the core and α particle, respectively, and

$$V_{QQ}=\sum_{\lambda}\kappa_\lambda\sum_{m=-\lambda}^{\lambda}(-1)^m Q^{\lambda}_m(\mathbf{r})Q^{\lambda}_{C-m}(\Omega) \tag{3}$$

is the multipole-multipole particle-core interaction. The coupling constants κ_λ in Eq. (3) are determined from the underlying particle-particle interaction.

The principal dynamical variables in this model are the α-core relative coordinate vector $\boldsymbol{r}\equiv\boldsymbol{R}_\alpha-\boldsymbol{R}_C$, the orientation $\boldsymbol{\Omega}$ (given, e.g., by the Euler angles) of the intrinsic core reference system with respect to the laboratory reference system, and the corresponding conjugate momenta $\boldsymbol{p}$ and $\boldsymbol{J}_C$, the latter being the core angular momentum. The individual intrinsic coordinates of the core and the α particle are ignored, but their intrinsic states can be included in the formulation if necessary. If we choose T_α to be the relative kinetic energy of (the center of mass of) the α particle and the core, then H_A is the intrinsic Hamiltonian of the nucleus A.

The multipole moment of multipolarity λ of the α-particle orbital entering Eq. (3) is defined as

$$Q^{\lambda}_m(\mathbf{r})=f_\lambda(r)\sqrt{\frac{4\pi}{2\lambda+1}}Y_{\lambda m}(\hat{r}), \tag{4}$$

where $f_\lambda(r)$ is the corresponding radial form factor. As a consequence of the rotational invariance of H_A, the form factor $f_\lambda(r)$ must be entirely independent of angles. The orientation-dependent core 2^λ-pole moment is given by

$$Q^{\lambda}_{Cm}(\boldsymbol{\Omega})=Q^{\lambda}_C\mathcal{D}^{\lambda *}_{m0}(\boldsymbol{\Omega}), \tag{5}$$

where the (electric) 2^λ-pole moment Q^{λ}_C for a uniform (charge) distribution with charge radius R_C is

$$Q^{\lambda}_C=2\left(\frac{3Z_C}{4\pi R_C}\right)\int r^\lambda P_\lambda(\cos\theta)d^3r. \tag{6}$$

The formulation in terms of a multipole-multipole force as in Eq. (2) can be shown to be equivalent to using an axially deformed intrinsic α-core potential with the symmetry axis coinciding with the symmetry axis of the core (i.e., the daughter nucleus). This potential generates single-particle α orbitals analogous to the Nilsson nucleon orbitals [33] corrected for the Coriolis force. Since one is interested in the wave functions in the laboratory system, the entire calculation is carried out in the laboratory reference frame. As the

interaction is expressed in terms of multipole-multipole operators, the orientation dependence of the interaction presents no further problems.

The intrinsic α-core optical potential $V(\mathbf{r},\mathbf{\Omega})$ may be approximated by the deformed WS potential

$$V(\mathbf{r},\theta)=\frac{V_{\rm WS}}{1+\exp\{[r-R(\theta)]/a_{\rm WS}\}}, \tag{7}$$

with the angle-dependent half-value radius $R(\theta)$ given by

$$R(\theta)=R_{\rm WS}\left\{1+\sum_{\lambda_{\rm min}}^{\lambda_{\rm max}}\beta_\lambda Y_{\lambda 0}(\cos\theta)\right\}. \tag{8}$$

Here θ is the angle between the position vector $\mathbf{r}$ of the α particle and the symmetry axis of the core. The form factor $f_\lambda(r)$ in Eq. (4) can be obtained in the first order from a Taylor expansion of the WS potential in β_λ, and the 2^λ-pole coupling constant κ_λ is given by the self-consistency relation [34]

$$\kappa_\lambda=\frac{1}{Z_{\rm C}}\frac{2\lambda+1}{\lambda+3}\frac{V_{\rm WS}R_{\rm WS}}{2a_{\rm WS}\langle r^\lambda\rangle_{\rm C}}. \tag{9}$$

B. Effect of shape coexistence

The problem presented by the data on neutron-deficient Pt, Hg, Pb, and Po isotopes [23] requires a modification of the model Hamiltonian. These nuclei are examples of shape coexistence showing rotational (and/or vibrational) bands which, although they have the same parity and signature, have quite different intrinsic structures and different deformation parameters. Transitions within the band show enhanced electric quadrupole rates, while electromagnetic transitions between members of different bands are strongly hindered.

In order to simulate the effect of shape coexistence, we assume that the excited (coexisting) band is coupled to the ground band by means of a monopole-monopole interaction which, by analogy with Eq. (2), can be written

$$\kappa_0 Q_0^{(0)}(\mathbf{r})Q_{\rm C}^{(0)}(\xi), \tag{10}$$

where the variable ξ denotes the quantum numbers of the core. In practice, we shall use the symbol ξ to distinguish between the coexisting band structures, i.e., the ground band ($\xi=0$) and the excited band ($\xi=1$).

According to Eq. (6) the monopole moment of the core is

$$Q_{\rm C}^{(0)}(\xi)=2\left[\frac{3Z_{\rm C}}{4\pi R_{\rm C}(\xi)}\right]\int P_0(\cos\theta)d^3r=2Z_{\rm C}R_{\rm C}(\xi)^2, \tag{11}$$

where, to a good approximation,

$$R_{\rm C}(\xi)^2=R(\xi)^2_{\rm WS}+7\pi^2 a(\xi)^2_{\rm WS} \tag{12}$$

(see, e.g., Appendix C of Ref. [35]). We see that the monopole moment of a WS distribution depends on both $R_{\rm WS}$ and $a_{\rm WS}$.

The strength of the monopole-monopole interaction should be determined from the observed bandhead energies and interband transitions. Because of conservation of angular momentum, only members of the same band having the same value of $\boldsymbol{J}_{\rm C}$ can be coupled via the monopole operator. This means that only the *radial* components of the mass and charge distributions can be affected by the monopole coupling. Consequently, in the present model only the WS parameters $R_{\rm WS}$ and $a_{\rm WS}$ can change as a direct result of the monopole transition. In the following, it has been assumed that the monopole transition is associated with the change of the radius $R_{\rm WS}$. Consequently, the coupling constant κ_0 and the form factor $f_0(r)$ to be used in conjunction with the monopole moment operator are given by

$$\kappa_0 f_0(r)\equiv\frac{\partial V(r,R_{\rm WS},a_{\rm WS})}{\partial R_{\rm WS}}\Delta R_{\rm WS}$$
$$=\frac{V_{\rm WS}}{a_{\rm WS}}\frac{\exp[(r-R_{\rm WS})/a_{\rm WS}]}{\{1+\exp[(r-R_{\rm WS})/a_{\rm WS}]\}^2}\Delta R_{\rm WS}, \tag{13}$$

where $R_{\rm WS}\equiv R_{\rm WS}(\xi=0)$ and $\Delta R_{\rm WS}\equiv R_{\rm WS}(\xi=1)-R_{\rm WS}(\xi=0)$. The dynamical cause of the assumed change $\Delta R_{\rm WS}$ of the radial shape of the potential that generates the α orbitals is not specified. As discussed in the Introduction, the predominant view at present of the underlying microscopic structure is that the coexisting configuration differs from that of the ground-state band by a two-nucleon-two-hole excitation [23].

It is a reasonable expectation that an α particle in an $\ell=0$ orbit surrounding the core in its 0^+ ground state may interact with the core and excite it to its next 0^+ state, and that such a change of the core state should also have consequences for the self-consistent α-core potential. The models proposed here are primarily constructed to satisfy these expectations qualitatively and to serve as a starting point for more quantitative approaches. The validity of the quantitative implementation of these ideas should then of course be subjected to severe tests and critically examined. The calculations presented here should be viewed as the first step in this direction.

C. Calculation of the decay rate

We now define a model Hamiltonian H_0 as

$$H_0=H_{\rm C}+H_\alpha+T_\alpha+\theta(R_{\rm b}-r)U(r)+\theta(r-R_{\rm b})U_{\rm b}+V_{QQ}, \tag{14}$$

where the last term, the multipole-multipole interaction, is given by Eq. (3). Note that the monopole term ($\lambda=0$) is also included. The α-core potential here is constant $U=U_{\rm b}$, for $r\geqslant R_{\rm b}$, $R_{\rm b}$ being the barrier radius. Therefore, H_0 may have bound states ϕ_{E_0} with energies in the interval $0<E_0\leqslant U_{\rm b}$. These states may be used as ''initial states'' in a process leading to eigenstates Ψ_E of the true Hamiltonian, Eq. (2), in accordance with the formalism of Refs. [9,10]. It is to be noted that the energy of the bound state, E_0, is not exactly equal to the energy of the α-particle resonance, E, the latter being associated with the real part of the pole in a matrix element of the full Green's function [9]. However, as discussed in Ref. [36], the resonance shift $\Delta E=E-E_0$ is extremely small and can be ignored in the process of readjust-

ing the depth of the potential well to reproduce experimental Q value (see below). Therefore, in the following we put $E_0 = E$. Since the true α-particle states Ψ_E are unbound and represented asymptotically by free outgoing Coulomb waves, they describe the decay of the initial state ϕ_{E_0}.

The solutions to $H_0\phi_M^I = E\phi_M^I$ with well-defined I and M are obtained by diagonalizing H_0 in the weak-coupling basis

$$\phi^{(\ell J_C)I}_{(nK_C\xi)M}(\mathbf{r},\Omega) = \sum_m \langle \ell, m, J_C, M-m | I, M\rangle \times [\chi_{n\ell m}(\mathbf{r}) X^{J_C M_C}_{K_C\xi}(\Omega)]^I_M , \quad (15)$$

resulting in coefficients $a^{K_C\zeta I}_{n\ell J_C\xi}$. Here $\chi_{n\ell m}(\mathbf{r})$ is the wave function of the α orbital and $X^{J_C}_{K_C\xi M_C}$ is a wave function of the core Hamiltonian corresponding to the diabatic configuration ξ [the quantum number ξ introduced in Sec. II B distinguishes between the ground band ($\xi=0$) and the coexisting excited band ($\xi=1$)]. The quantum number K_C is the projection of the core spin $\mathbf{J}_C$ on the symmetry axis of the core, and ζ stands for other quantum numbers labeling the core states.

Using the formalism of Refs. [9,10] with the model eigenstates ϕ_M^I as initial states, the (partial) decay rate, $\omega_{J_C K_C \zeta} = \Gamma_{J_C K_C \zeta}/\hbar$, for populating the daughter state (labeled by its spin J_C, bandhead spin K_C, and band label ζ) is given by

$$\omega_{J_C K_C \zeta} = \frac{4\mu}{\hbar^3 k_{J_C K_C}} \sum_{n\ell\xi} |a^{K_C\zeta I}_{n\ell J_C\xi}|^2 |T_{n\ell\xi}|^2, \quad (16)$$

where

$$T_{n\ell\xi} = \int_{R_b}^{\infty} F_\ell(r) V(r) u_{n\ell\xi}(r) dr \quad (17)$$

is the α-transition amplitude (''transmission coefficient'') in the $(n\ell)$ channel. In Eq. (17), $V(r) = \{U(r) - U_b\}\theta(r - R_b)$ is the interaction causing the decay and $u_{n\ell\xi}(r)$ is the radial wave function of the α particle. It is generated in a spherical WS potential which is different in the two bands because R_{WS} depends on ξ. [As discussed in the following section, the label ξ distinguishes between the *diabatic* (noninteracting) core states while ζ stands for the physical *adiabatic* (mixed) core states.] The function $F_\ell(r)$ represents the regular scattering radial wave function of the Hamiltonian $T+V+U_b$. In practice, F_ℓ can be well approximated by the regular Coulomb wave function; the associated error on the decay width does not exceed 10% [36]. The influence of deformations of various multipolarities is incorporated through the coefficients $a^{K_C\zeta I}_{n\ell J_C\xi}$.

The model described here, or its nearest predecessors, has previously been applied to a variety of nuclei with masses in the range $200 < A < 230$. To interpret and judge the results one must understand how the analysis is done. Initially the Hamiltonian (14) is diagonalized assuming that one of the eigenvectors $\{a^{K_C\zeta I}_{n\ell J_C\xi}\}$ is the one that corresponds to the ''ground state'' of the parent nucleus. It must be elaborated that although only one solution is thought to be physically relevant, it will be seen that this choice is not always obvious when performing calculations. This is an important point that will be taken up more thoroughly in Sec. IV C. The solutions are labeled according to their relative energy after diagonalization, but before their individual tuning to adjust the potential depth. Diagonalization and readjusting is performed until the correct decay energy Q_α is obtained for a particular solution. When this solution has the correct decay energy, the relative feedings to excited states of the daughter nucleus are calculated.

For computational reasons we usually restrict the α orbitals to one or two major shells, viz., those compatible with the assumed single-nucleon constituents of the α particle according to the so-called oscillator rule [32],

$$N_\alpha = N_{p_1} + N_{p_2} + N_{n_1} + N_{n_2}. \quad (18)$$

In deformed nuclei this rule loses precision because the single-nucleon orbitals there have components from several spherical shells, but it remains useful as a rule of thumb for setting the major quantum number N_α. The oscillator rule is also an approximate way of satisfying the Pauli principle for the nucleons in the α particle with respect to those in the core. The assumption made here is that the formation has already taken place when the decay occurs; it is an α particle that penetrates the Coulomb barrier, not four separate nucleons which come together during or after the penetration.

D. Mixing of core states

A model of how bands of different kinds can interact in a nucleus and give rise to modified bands with mixed properties was suggested by Dickmann and Dietrich [37] and later applied by several groups [38–40] for structure considerations. It has also been used by Wauters *et al.* [27] in α-decay analysis.

The two-band model assumes that the states of the even-even daughter nuclide $^{A-4}(Z-2)$ can be approximately described as belonging to either of two bands, the ''ground band'' and the ''intruder band.'' We need not go further into the physical nature of these states; we simply assume that they are eigenstates of a model core Hamiltonian H_{C_0} and have different and distinguishable properties. The ''true'' core Hamiltonian H_C differs from the model Hamiltonian H_{C_0} by an interaction $H_C - H_{C_0} \equiv V$ coupling the bands such that

$$\langle X^J_\xi | V | X^{J'}_{\xi'} \rangle = V_J \delta_{JJ'}(1 - \delta_{\xi\xi'}). \quad (19)$$

The ''true'' daughter states $X_{\zeta,J}$ are eigenstates of $H_C = H_{C_0} + V$; they are linear combinations of the model core states X^J_0 and X^J_1:

$$X_{\zeta,J} = \alpha_{\zeta,J} X^J_{\xi=0} + \beta_{\zeta,J} X^J_{\xi=1}, \quad \zeta = 0,1. \quad (20)$$

The interaction V is usually associated with the $E0$ transitions between spherical and deformed states in the core system. As discussed in, e.g., Ref. [39], the observed $E0$ transition strengths result from the mixing of states with different shapes.

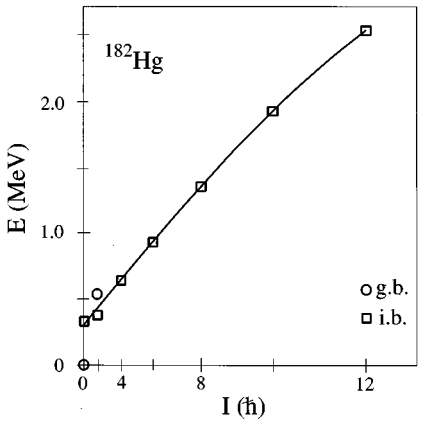

FIG. 1. Calculated diabatic excitation energies (solid line) as functions of $I(I+1)$ for the ground-band (g.b.) and well-deformed intruder band (i.b.) in ^{182}Hg. Experimental data are indicated by symbols.

The decay theory presented in the preceding sections describes how the ''true'' core states $\Psi_{n,J}$ are populated when an α particle in the parent nucleus makes a transition from a metastable state ϕ_M^I, a quasibound eigenstate of the model Hamiltonian H_0, Eq. (14), to the final state in which the core is represented by $\Psi_{\zeta,J}$ and the α particle is in outgoing state with appropriate wave number k_f. However, in developing the decay formalism, we have tacitly assumed that the core states are such that the matrix elements of the multipole operators can be calculated as if the core states are pure rotor (or pure vibrator) eigenfunctions. The actual values of the matrix elements are specified in terms of deformations which are input parameters for the calculation.

The amount of mixing, i.e., the parameters $\alpha_{\zeta,J}$ and $\beta_{\zeta,J}$, is calculated based on experimental data. We should clearly distinguish between the ''true'' core state labels $\zeta=0,\ 1$ and the labels $\xi=0,\ 1$ introduced in Sec. II B which define the diabatic (noninteracting) core states. The coefficients $a^{K_C\zeta I}_{n\not J_C\xi}$ which specify the solutions to the eigenvalue problem $H_0\phi_M^I=E\phi_M^I$ can then easily be expressed in terms of the mixing parameters $\alpha_{\zeta,J}$ and $\beta_{\zeta,J}$.

III. BAND MIXING

Band interactions V_J and mixing coeficients $\alpha_{\zeta,J}$ and $\beta_{\zeta,J}$ have been extracted for the daughter nuclei ^{176,178,180}Pt and ^{182,184,186}Hg using the two-level model of Sec. II D. Above spin $I=6$, the well-deformed prolate band becomes yrast in these nuclei [23]. The diabatic bands ($\xi=0$ and 1) can be parametrized using the standard expansion

$$E_{J,\xi}=A_\xi+B_\xi J(J+1)+C_\xi J^2(J+1)^2. \tag{21}$$

Because of the lack of experimental data, an assumption has been made that the interactions between the 0^+ states and the 2^+ states in ^{182,184}Hg are equal. The results of band-mixing calculations for ^{182}Hg are illustrated in Fig. 1 where the $I=6$–12 band members of the deformed intruder band were considered in the fit, Eq. (21). The resulting band-mixing parameters for all Pt and Hg nuclei considered in our study are listed in Table I.

TABLE I. Results of band mixing calculations. Experimental excitation energies have been taken from Ref. [44]. Numbers in brackets were obtained by assuming $V_{J_C}=V_0$ (see text). The mixing amplitude α_{J_C} [Eq. (20)] always corresponds to a weakly deformed (or spherical) structure. For instance, for the Hg isotopes α_{J_C} decreases from the value close to one at $J_C=0$ (oblate ground state) to small values at $J_C=4$ (prolate band becomes yrast).

Nucleus	J_C	Unperturbed energy (keV)	Experimental energy (keV)	$\lvert V\rvert$ (keV)	$\lvert\alpha_{J_C}\rvert$
^{186}Hg	0	16	0	90.0	0.985
		506.7	522.7		
	2	422.9	405.4	58.8	0.959
		603.7	621.1		
	4	1060.5	808.2	71.3	0.272
		828.3	1080.7		
^{184}Hg	0	19.8	0	83.9	0.973
		355.3	375.1		
	2	451.8	366.5	83.9	0.701
		449.1	534.4		
	4	1078.1	653.3	66.8	0.155
		663.8	1088.6		
^{182}Hg	0	23.4	0	84.5	0.964
		304.6	328 [a]		
	2	500.7	351.8	84.5	0.494
		399.8	548.6		
	4		613.2	[84.5]	0.0435
		616.9			
^{180}Pt	0	292	0	233.5	0.624
		186.7	478.7		
	2	741.6	153.3	265.5	0.411
		273.1	861.4		
	4	1186.6	410.8	219.8	0.273
		472.3	1248.1		
^{178}Pt	0	217.8	421.9	210.8	0.696
		204.1	0		
	2			[210.8]	[0.490]
		[288.5]	170.1		
	4			[210.8]	[0.257]
		[483.1]	427.1		
^{176}Pt	0	75.2	0	166.3	0.90
		367.8	443 [a]		
	2		263.9	[166.3]	[0.703]
		[449.8]			
	4		564.1	[166.3]	[0.325]
		[638.4]			

[a] From Ref. [26].

For ^{190,192,194}Pb, the band-mixing parameters were found in Ref. [38]; for completeness they are shown in Table II. As the ground states of the Pb isotopes are spherical, a deformation of $\beta_2=0.01$ was assigned to the ground band, necessary to perform the calculation.

IV. CHOICE OF PHENOMENOLOGICAL PARAMETERS

A. Results

As was discussed earlier in Sec. II C, only one eigenstate of Hamiltonian (14) is considered as the physical solution

TABLE II. Band-mixing parameters for ^{190,192,194}Pb taken from Ref. [38].

Nucleus	J_C	Unperturbed energies (keV)	Experimental energies (keV)	$\|V\|$ (keV)	$\|\alpha_{J_C}\|$
^{194}Pb	0	2.7	0	50.9	0.997
		927.9	930.6		
	2	1066.1	965.0	157	0.834
		1207	1308.2		
^{192}Pb	0	3.5	0	52.0	0.995
		764.9	768.5		
	2	1066.9	853.8	191	0.668
		1025	1237.8		
^{190}Pb	0	>9	0	>80	<0.99
		<649	658		
	2	871	773	[191]	0.457
		1078.1	[1176]		

representing the ground state of the α-parent nucleus. Initially, the calculations were performed using WS parameters found by DeVries in the α-scattering experiments on ^{208}Pb [41] (set A: $r_{WS}=1.32$ fm, $a_{WS}=0.65$ fm). Subsequently, for each nucleus, the two parameters, i.e., the quadrupole coupling strength κ_2 and the monopole ''radial shift'' ΔR_{WS}, were adjusted until the theoretical relative intensities best matched experimental values (local fit). We found that these parameters fall into separate ranges for each group of isotopes. Therefore the next step was to calculate a global least squares fit with one set of parameters for all the isotopes of each element. The resulting relative intensities are listed in Table III. The associated κ_2 and ΔR_{WS} parameter sets are listed in Table IV.

For the Hg decays, the quadrupole coupling strength κ_2 obtained in the local fit has a fairly similar value for all three decays. However, ΔR_{WS} becomes very small, in order to best fit the decay data of ^{180}Hg. This might be due to the fact that the ground state of the daughter nucleus, ^{176}Pt, has a different deformation as compared to the 2^+ and 4^+ yrast states. Indeed, according to Ref. [42], the ground state of ^{176}Pt is triaxial and not oblate as has been assumed in our calculations. Consequently, the global fit for the Hg decays is in worse agreement with experiment than for the other isotopic chains considered. As mentioned above, the α-rotor model does not predict half-lives (i.e., absolute α-decay widths) correctly (neglected α-formation probability in the assumed parent state ϕ_M^I, violated Pauli principle), but is able to reproduce the relative intensities to a rather good accuracy.

B. Effects of band mixing on relative intensities

The effect of configuration mixing at the 2^+ states on the α-decay relative intensities ^{180,182,184}Hg is shown in Table V. The range of mixing amplitudes used in the calculation was varied for the different isotopes around the experimentally deduced values displayed in Table I. It is to be noted that because of the normalization condition in Eq. (1) the relative intensities to other states with $J_C \neq 2$ vary as well.

According to calculations, for the α decay of ^{188}Pb and ^{190}Pb, the effect due to shape mixing is rather weak. However, in the case of the $^{186}\text{Pb}\rightarrow{}^{182}$Hg α decay, the relative intensities are quite sensitive to shape mixing. This is further illustrated in Fig. 2. The α-decay intensity to the 2_1^+ state decreases with increasing mixing while the intensity to the 2_2^+ state increases. This is not surprising since the increased ground-state-band-like component in the 2_1^+ state is expected to enhance the relative feeding and, by the same token, it should result in a stronger hindrance for the α decay to the 2_2^+ state. In Ref. [43] this observation has been dis-

TABLE III. Calculated α-decay relative intensities (in %) obtained in a local and global fit (see text). Experimental relative intensities (I_{expt}) [26,27] are included for comparison.

Daughter	J_C^π	I_{expt}	I_{th}^{local}	I_{th}^{global}
^{186}Hg	2_1^+	8.4×10^{-2}	8.4×10^{-2}	1.1×10^{-1}
	0_2^+	1.5×10^{-2}	1.5×10^{-2}	1.0×10^{-2}
	2_2^+		1.4×10^{-3}	1.2×10^{-3}
^{184}Hg	2_1^+	6.0×10^{-2}	6.0×10^{-2}	1.3×10^{-1}
	0_2^+	9.5×10^{-2}	9.5×10^{-2}	1.7×10^{-1}
	2_2^+		1.1×10^{-2}	2.2×10^{-2}
^{182}Hg	2_1^+	$<7\times10^{-2}$	7.0×10^{-2}	4.3×10^{-3}
	0_2^+	2×10^{-1}	2.0×10^{-1}	2.5×10^{-1}
	2_2^+		2.8×10^{-1}	2.3×10^{-1}
^{180}Pt	2_1^+	4.2×10^{-1}	4.2×10^{-1}	6.4×10^{-1}
	0_2^+	1.6×10^{-1}	1.6×10^{-1}	1.5×10^{-2}
^{178}Pt	2_1^+	8.4×10^{-1}	6.7×10^{-1}	2.1×10^{-1}
	0_2^+	3.4×10^{-1}	1.8×10^{-1}	5.8×10^{-2}
^{176}Pt	2_1^+	1.0×10^{-1}	2.7×10^{-1}	7.0×10^{-1}
	0_2^+	7.8×10^{-2}	2.5×10^{-1}	9.3×10^{-1}
^{194}Pb	2_1^+	$<3.6\times10^{-4}$	3.7×10^{-4}	2.8×10^{-4}
	0_2^+	1.3×10^{-3}	1.7×10^{-3}	1.3×10^{-3}
	2_2^+		3.5×10^{-5}	2.7×10^{-5}
^{192}Pb	2_1^+	8.4×10^{-3}	8.4×10^{-3}	1.3×10^{-3}
	0_2^+	2.2×10^{-2}	2.4×10^{-2}	3.2×10^{-2}
	2_2^+		4.6×10^{-4}	1.6×10^{-4}
^{190}Pb	2_1^+		3.0×10^{-2}	6.1×10^{-3}
	0_2^+	2.4×10^{-1}	3.0×10^{-1}	2.6×10^{-1}
	2_2^+		2.3×10^{-3}	9.7×10^{-4}

TABLE IV. The coupling constants κ_2 and ΔR_{WS} obtained in local and global fit performed in this work.

Parent nucleus	κ_2 (MeV/fm^2)	ΔR_{WS} (fm)
^{190}Pb	0.029	0.030
^{188}Pb	0.024	0.015
^{186}Pb	0.045	0.047
Global Pb	0.037	0.035
^{184}Hg	0.028	0.161
^{182}Hg	0.016	0.077
^{180}Hg	0.010	0.001
Global Hg	0.052	0.041
^{198}Po	0.025	0.110
^{196}Po	0.033	0.142
^{194}Po	0.020	0.126
Global Po	0.035	0.118

TABLE V. Relative intensities for α-decay to low-lying excited states in ^{182,184,186}Hg as functions of a mixing probability $|\alpha|^2$ in the 2_1^+ state.

			^{186}Hg		
$J_\zeta^\pi \backslash \|\alpha_2\|^2$	0.50	0.60	0.70	0.80	0.90
2_1^+	1.16×10^{-1}	1.14×10^{-1}	1.08×10^{-1}	1.03×10^{-1}	1.04×10^{-1}
4_1^+	5.59×10^{-6}	2.62×10^{-6}	1.21×10^{-7}	1.76×10^{-6}	1.17×10^{-5}
0_2^+	4.48×10^{-2}	2.87×10^{-2}	1.93×10^{-2}	1.38×10^{-2}	1.05×10^{-2}
2_2^+	1.37×10^{-3}	1.49×10^{-3}	1.48×10^{-3}	1.40×10^{-3}	1.26×10^{-3}
			^{184}Hg		
$J_\zeta^\pi \backslash \|\alpha_2\|^2$	0.50	0.60	0.70	0.80	0.90
2_1^+	1.31×10^{-1}	1.58×10^{-1}	1.90×10^{-1}	2.26×10^{-1}	2.71×10^{-1}
4_1^+	7.13×10^{-4}	8.05×10^{-4}	8.20×10^{-4}	7.23×10^{-4}	4.43×10^{-4}
0_2^+	1.62×10^{-1}	1.37×10^{-1}	1.19×10^{-1}	1.04×10^{-1}	9.22×10^{-2}
2_2^+	2.16×10^{-2}	1.67×10^{-2}	1.33×10^{-2}	1.08×10^{-2}	8.65×10^{-3}
			^{182}Hg		
$J_\zeta^\pi \backslash \|\alpha_2\|^2$	0.50	0.60	0.70	0.80	0.90
2_1^+	4.43×10^{-2}	6.85×10^{-2}	1.03×10^{-1}	1.47×10^{-1}	1.98×10^{-1}
4_1^+	8.09×10^{-5}	1.15×10^{-3}	1.47×10^{-3}	1.78×10^{-3}	1.96×10^{-3}
0_2^+	2.49×10^{-1}	2.83×10^{-1}	2.92×10^{-1}	2.90×10^{-1}	2.81×10^{-1}
2_2^+	2.23×10^{-1}	1.35×10^{-1}	9.33×10^{-2}	6.87×10^{-2}	5.29×10^{-2}

cussed in terms of the variation of α-decay hindrance factors to 2_1^+ states in ^{182,184,186}Hg.

As illustrated in Fig. 3 for the α decay of ^{198}Po, the relative intensities of the Po decays do not exhibit a significant variation with shape mixing. This might be due to the fact that in our calculations the ground-state structure of Pb was assumed to be spherical (see Sec. III) and the intruder configuration very weakly deformed.

C. Choice of Woods-Saxon parameters

To investigate the influence of the optical model parameters on relative intensities, a second set of WS parameters proposed in Ref [12] (set B: $r_{\rm WS}=1.05$ fm and $a_{\rm WS}=0.70$ fm) was employed. The main difference between the sets A and B is a much smaller WS radius in set B.

A least squares minimization was performed, for a set of isotopes, for both parameter sets to establish optimal values of κ_2 and $\Delta R_{\rm WS}$. For the intermediate values of $r_{\rm WS}$, the calculations were carried out by linearly interpolating other parameters between the two limiting ''best-fit'' values. For the Pb nuclei, the parameters κ_2 and $\Delta R_{\rm WS}$ were found to change very little. The variation of the relative intensities for the Pb decays as a function of the WS parameters is shown in Fig. 4. The relative intensities show relatively little variation as a function of WS parameters. However, the calculations show that when using WS parameters close to those of set B, the better agreement with experiment is obtained for the eigenstate of Hamiltonian (14) corresponding to the solution ''2'' rather than the solution ''3,'' the latter being optimal for the Pb decays using A parametrization. This behavior is illustrated in Fig. 5.

Part of the analysis in this work has been concerned with the choice of a particular solution. Fortunately, in most cases

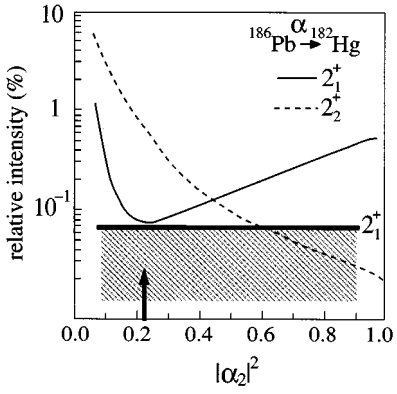

FIG. 2. Relative intensities of ^{186}Pb decay versus the mixing amplitude $|\alpha|_2$ of the 2^+ states in ^{182}Hg. Lines represent calculation. The arrow on the abscissa shows the calculated mixing amplitude from Table I. The upper limit on the experimental relative intensity for the 2_1^+ feeding is also shown. In the calculations, the parameters κ_2 and $\Delta R_{\rm WS}$ obtained from the local fit (Table IV) were used.

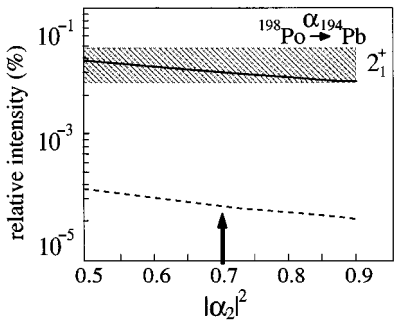

FIG. 3. Similar as in Fig. 2 except for the ^{198}Po decay. The gray bar stands for the experimental value; its width corresponds to the experimental uncertainty.

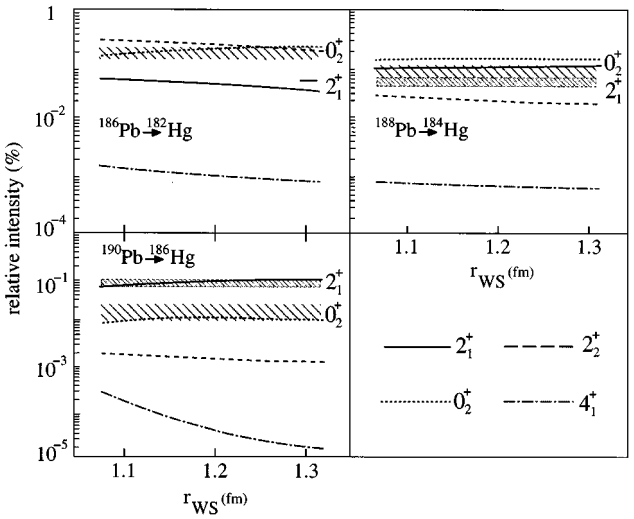

FIG. 4. Dependence of the relative intensities in the α decay of ^{186,188,190}Pb on the radius r_{WS} of the optical model potential.

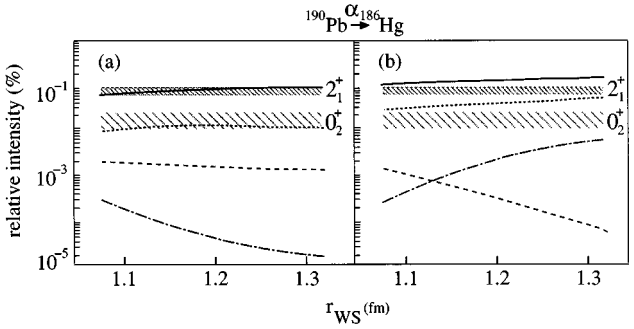

FIG. 5. Same as in Fig. 4 except for the two solutions for ^{190}Pb, namely, solution 3 (a) and solution 2 (b).

only one solution provides a reasonable fit of the experimental data. For instance, for the ^{186}Pb decay, only solution number ''3'' can match experimental relative intensities. Moreover, this choice is supported by the fact that this solution is rather sensitive to the mixing between 2^+ states, in agreement with what is observed experimentally [26,43]. Similarly, solution ''3'' agrees best with experimental data for the α decays of ^{188}Pb and ^{190}Pb. On the other hand, for the Po decays, the optimal solutions vary from nucleus to nucleus.

V. CONCLUSION

In this paper the modified two-potential approach to the decay of a quasistationary state has been used in conjunction with the particle-plus-rotor model to study fine structure in the α decay of even-even neutron-deficient nuclei in the lead region. These nuclei are known to exhibit shape coexistence between the ground-state band and an excited band having different deformation. The effect of configuration mixing was incorporated in the particle-core formalism. By taking experimental band interaction, all experimental relative intensities were reproduced within one order of magnitude, except for ^{180}Hg. This probably can be explained in terms of a triaxial ground-state and low-spin shape change in the daughter nucleus ^{176}Pt.

Our analysis demonstrates that configuration mixing has a significant effect on the relative intensities, except for the Po decays. Finally the influence of the WS parameters was studied. The Hg and Pb decays were found to be rather stable against the variation of the optical model parameters. For the Po isotopes, however, considerable changes in multipole coupling strengths were needed in order to fit the experimental relative intensities. Interestingly, a change in the radius of the optical model potential, while having a significant effect on the calculated α-decay half-life, had considerably less effect on the relative intensities.

Our primary concern for this work was to show the validity and applicability of the α-particle-plus rotor model to calculate fine structure in the α decay to nuclei that exhibit shape coexistence. We expect that the model can be used to calculate the relative intensities in α decay of nuclei further away from the $Z=82$ shell closure where fine structure has been observed, e.g., Pt and Rn decays.

ACKNOWLEDGMENTS

Useful discussions with G. Dracoulis are gratefully acknowledged. Nuclear physics research at The University of Tennessee is supported by the U.S. Department of Energy through Contracts Nos. DE-FG05-87ER40361 and DE-FG02-96ER40963. The research was partially sponsored by the Oak Ridge National Laboratory, managed by Lockheed-Martin Energy Research Corporation for the U.S. Department of Energy under Contract No. DE-AC05-96OR22464. The Joint Institute for Heavy Ion Research has as member institutions the University of Tennessee, Vanderbilt University, and the Oak Ridge National Laboratory; it is supported by the members and by the U.S. Department of Energy through Contract No. DE-FG05-87ER40361 with the University of Tennessee.

[1] G. Gamow, Z. Phys. **51**, 204 (1928).
[2] E. U. Condon and R. W. Gurney, Nature (London) **122**, 439 (1928).
[3] J. O. Rasmussen, Phys. Rev. **113**, 1593 (1959).
[4] G. Igo, Phys. Rev. **115**, 1665 (1959).
[5] H. J. Mang, Phys. Rev. **119**, 1069 (1960).
[6] R. G. Lovas, R. J. Liotta, A. Insolia, K. Varga, and D. S. Delion, Phys. Rep. (to be published).
[7] S. G. Kadmenskiĭ and V. E. Kalechtis, Sov. J. Nucl. Phys. **12**, 37 (1971).
[8] J. Schlitter, Nucl. Phys. **A211**, 96 (1973).
[9] S. A. Gurvitz and G. Kalbermann, Phys. Rev. Lett. **59**, 262 (1987).
[10] S. A. Gurvitz, Phys. Rev. A **38**, 1747 (1988).
[11] T. Berggren and P. Olanders, Nucl. Phys. **A473**, 189 (1987).
[12] T. Berggren, Phys. Rev. C **50**, 2494 (1994).

[13] B. Buck, A. C. Merchant, and S. M. Perez, J. Phys. G **17**, 1223 (1991); **17**, L91 (1991).
[14] P. O. Fröman, Mat. Fys. Medd. K. Dan. Vidensk. Selsk. **1**, 1 (1957).
[15] T. L. Stewart, M. W. Kermode, D. J. Beachey, N. Rowley, I. S. Grant, and A. T. Kruppa, Phys. Rev. Lett. **77**, 36 (1996).
[16] A. Insolia, R. J. Liotta, and E. Maglione, Europhys. Lett. **7**, 209 (1988).
[17] K. Varga, R. G. Lovas, and R. J. Liotta, Nucl. Phys. **A550**, 421 (1992).
[18] K. Varga, R. G. Lovas, and R. J. Liotta, Z. Phys. A **349**, 345 (1994).
[19] A. Insolia, P. Curutchet, R. J. Liotta, and D. S. Delion, Phys. Rev. C **44**, 545 (1991).
[20] D. S. Delion, A. Insolia, and R. J. Liotta, Phys. Rev. C **46**, 1346 (1992).
[21] D. S. Delion, A. Insolia, and R. J. Liotta, Phys. Rev. C **46**, 884 (1992).
[22] D. S. Delion, A. Insolia, and R. J. Liotta, Phys. Rev. C **49**, 3024 (1994).
[23] J. L. Wood, K. Heyde, W. Nazarewicz, M. Huyse, and P. Van Duppen, Phys. Rep. **215**, 101 (1992).
[24] K. Heyde, J. Jolie, J. Moreau, J. Ryckebusch, M. Waroquier, P. Van Duppen, M. Huyse, and J. L. Wood, Nucl. Phys. **A466**, 189 (1987).
[25] N. Bijnens, P. Decrock, S. Franchoo, M. Gaelens, M. Huyse, H.-Y. Hwang, I. Reusen, J. Szerypo, J. von Schwarzenberg, J. Wauters, J. G. Correia, A. Jokinen, P. Van Duppen, and the ISOLDE Collaboration, Phys. Rev. Lett. **75**, 4571 (1995).
[26] J. Wauters, N. Bijnens, P. Dendooven, M. Huyse, H. -Y. Hwang, G. Reusen, J. von Schwarzenberg, P. Van Duppen, R. Kirchner, E. Roeckl, and the ISOLDE Collaboration, Phys. Rev. Lett. **72**, 1329 (1994).
[27] J. Wauters, N. Bijnens, H. Folger, M. Huyse, H. -Y. Hwang, R. Kirchner, J. von Schwarzenberg, and P. Van Duppen, Phys. Rev. C **50**, 2768 (1994).
[28] D. S. Delion, A. Florescu, M. Huyse, J. Wauters, P. Van Duppen, A. Insolia, and R. J. Liotta, Phys. Rev. Lett. **74**, 3939 (1994).
[29] D. S. Delion, A. Florescu, M. Huyse, J. Wauters, P. Van Duppen, ISOLDE Collaboration, A. Insolia, and R. J. Liotta, Phys. Rev. C **54**, 1169 (1996).
[30] E. Van Walle, J. Wouters, D. Vandeplassche, N. Severijns, and L. Vanneste, Hyperfine Interact. **22**, 507 (1985).
[31] T. Berggren, Hyperfine Interact. **43**, 407 (1988).
[32] T. Berggren, Hyperfine Interact. **75**, 401 (1992).
[33] S. G. Nilsson, Mat. Fys. Medd. K. Dan. Vidensk. Selsk. **29**, 16 (1959).
[34] A. Bohr and B. Mottelson, *Nuclear Structure* (Benjamin, New York, 1975), Vol. II.
[35] L.R.B. Elton, *Nuclear Sizes* (Oxford University Press, Oxford, 1961).
[36] S. Åberg, P.B. Semmes, and W. Nazarewicz, Phys. Rev. C (to be published).
[37] F. Dickmann and K. Dietrich, Z. Phys. A **271**, 417 (1974).
[38] P. Van Duppen, M. Huyse, and J. L. Wood, J. Phys. G **16**, 441 (1990).
[39] K. Heyde and R. A. Meyer, Phys. Rev. C **37**, 2170 (1988).
[40] G. D. Dracoulis, Phys. Rev. C **49**, 3324 (1994).
[41] R. M. DeVries, J. S. Lilley, and M. A. Franey, Phys. Rev. Lett. **37**, 4481 (1976).
[42] B. Cederwall, R. Wyss, A. Johnson, J. Nyberg, B. Fant, R. Chapman, D. Clarke, F. Khazaie, J. C. Lisle, J. N. Mo, J. Simpson, and I. Thorslund, Z. Phys. A **337**, 283 (1990).
[43] J. D. Richards, C. R. Bingham, Y. A. Akovali, J. A. Becker, E. A. Henry, P. Joshi, J. Kormicki, P. F. Mantica, K. S. Toth, J. Wauters, and E. F. Zganjar, Phys. Rev. C **54**, 2041 (1996).
[44] R.B. Firestone, in *Table of Isotopes*, edited by V.S. Shirley (Wiley, New York, 1996).